A Semigeostrophic Eady-Wave Frontal Model Incorporating Momentum Diffusion. Part II: Kinetic Energy and Enstrophy Dissipation

WILLIAM BLUMEN

Department of Astrophysical, Planetary, and Atmospheric Sciences, University of Colorado, Boulder, Colorado

(Manuscript received 14 November 1989, in final form 15 May 1990)

ABSTRACT

Momentum diffusion has been introduced into a semigeostrophic Eady-wave frontal model by Blumen (Part I). This model is used to determine the kinetic energy and enstrophy dissipations within a frontal zone that extends from the ground to a midtropospheric level. The largest amount of kinetic energy dissipation occurs when a relatively small nondimensional eddy viscosity coefficient is used, and the front attains an equilibrated state—a balance between unstable growth and momentum diffusion. The magnitude of kinetic energy dissipation ranges from about 50 to 250 W m^{-2} for parameter values that characterize surface-based fronts. These values are comparable to the 75 W m^{-2} determined by Kennedy and Shapiro from observations in an upper-level front, but are about one to two orders of magnitude larger than previous estimates of kinetic energy dissipated locally in clear-air turbulence zones and in the planetary boundary layer. An estimate of global kinetic energy dissipation in the planetary boundary layer is provided. A comparison establishes that fronts may make a relatively large contribution to the dissipation occurring during the life cycle of a cyclone, but the global contribution is less than that associated with the planetary boundary layer.

Frontal equilibration is characterized by a balance between production and dissipation of enstrophy. However, as frontolysis sets in, the dissipation of enstrophy becomes the dominant feature. Finally, it is noted that the physical process associated with the cascade of energy and enstrophy to dissipative scales differs from the cascade process described by the theory of homogeneous turbulence, and a different spectral decay law is realized.

1. Introduction

Most of what is known about the fine-scale structure of surface cold fronts with sharply defined transition zones, the order of hundreds of meters to a few kilometers, is based on observations from instrumented meteorological towers. Among the characteristics observed in the studies by Young and Johnson (1984), Shapiro (1984), and Brümmer (1988), for example, are large magnitude up-and-down-drafts, large horizontal and vertical shears of the horizontal wind, significant variability of the temperatures measured by fast response thermometers, and evidence to suggest strong mixing within the zone itself. A model that takes account of relatively extreme variability of both motions and temperatures within frontal zones is yet to be developed. The problem is more than one of grid resolution: shear and convective instabilities both in the planetary boundary layer and in the free atmosphere, and concomitant turbulent mixing need to be represented as natural processes, rather than as parameterizations. These phenomena have been subject to intensive investigation by both laboratory and numerical model experimentation, and by development of phenomenological theories, e.g., Thorpe (1987) and Lesieur (1987). Current research progress indicates that it would be premature to anticipate that realistic mesoscale models, which take account of microscale features of frontal (or other) transitional zones, will be developed for operational or even research purposes in the near future. At present it appears that the only option is to rely on a physical parameterization of turbulent mixing within a frontal transition zone.

The frontal model presented in Part I (Blumen 1990) represents an attempt to parameterize the effects of turbulent mixing: frontal collapse is prevented and momentum diffusion ultimately balances unstable baroclinic amplitude growth. This model appears to capture physical aspects of frontogenesis and equilibration, but it is not without limitations. In particular, it is based on semigeostrophic theory, so that ageostrophic motions within the frontal zone are not captured. Other omissions are the alteration in the vertical structure of the front as it equilibrates (Nakamura and Held 1989), and the generation of internal gravity waves during the frontogenetical stage (Gall et al. 1987, 1988). Nonetheless, semigeostrophic frontal models do tend to capture the essence of significant physical features that characterize observed fronts. Some comparisons between theory and observation have been reported, for example, by Blumen (1980) and by Hoskins (1982, and references therein).

Corresponding author address: Dr. William Blumen, Center for Atmospheric Theory and Analysis, University of Colorado, Campus Box 391, Boulder, CO 80309-0391.

Dissipation occurs to various degrees as a front evolves from a nascent wave to frontolysis. Some dissipation of kinetic energy will occur in the planetary boundary layer, and some will occur at higher altitudes. The latter mechanism is associated with turbulence generated by convection and instabilities of internal gravity waves, whose source of energy can be related to frontal forcing at lower levels. Finally, turbulence within the frontal zone makes a contribution to kinetic energy dissipation.

The present study only takes account of kinetic energy dissipation within the transition region of a front, which extends from the ground surface to a midtropospheric level. The model of Part I will be used to provide theoretical estimates of dissipation that may be compared to other dissipative mechanisms, frontal or not. For example, Hess (1959, §19.3) estimated the dissipation of kinetic energy in the planetary boundary layer to be the order of 1–5 W m^{-2}, based on an evaluation using the Ekman solution for the velocity profile. Estimates of dissipation in zones of clear air turbulence, in the upper troposphere and lower stratosphere, are often based on use of observational data acquired by aircraft together with an inertial range assumption of the energy transfer to dissipative scales. Most estimates of dissipation in clear-air turbulence zones are also the order of 1–5 W m^{-2} over depths of a few kilometers, e.g., Trout and Panofsky (1969); Lilly and Lester (1974) and Kennedy and Shapiro (1975).

More recently Kennedy and Shapiro (1980) used aircraft data to examine dissipation of kinetic energy within an upper-level front. The average dissipation rate found within an upper tropospheric front is approximately 3×10^{-2} m^2 s^{-3}. The frontal zone extends over a depth of about 5 km and the mean density in this layer is about 0.5 kg m^{-3}, so that the dissipation of kinetic energy is approximately 75 W m^{-2}. This dissipation is one to two orders of magnitude larger than values that have been associated with both clear air turbulence and the planetary boundary layer.

The estimates provided above suggest that fronts may provide local sinks of dissipation that need to be considered in atmospheric models that take account of other dissipative mechanisms. There do not appear to be any estimates of low-level frontal dissipation that would complement the estimate provided by Kennedy and Shapiro (1980). The present approach provides estimates of kinetic energy dissipation in surface-based fronts from model solutions presented in Part I. These estimates support the observational study of Kennedy and Shapiro: in fact, a model frontal zone that extends through a depth of about 5 km can provide a kinetic energy dissipation of the order of 50–250 W m^{-2}.

It may seem inappropriate to make use of the present model solutions to the dissipation problem in view of the fact that the characteristic along-front velocity v is the order of 100 m s^{-1}. However, only spatial gradients of the velocity appear in the present analysis, and the values predicted by the model do not exceed characteristic atmospheric values. For example, the model provides a cross-front shear of magnitude

$$\frac{\partial v}{\partial x} \approx \frac{200 \text{ m s}^{-1}}{200 \times 10^3 \text{ m}} = 10^{-3} \text{ s}^{-1}.$$

A comparable atmospheric value might be

$$\frac{\partial v}{\partial x} \approx \frac{2 \text{ m s}^{-1}}{2 \times 10^3 \text{ m}} = 10^{-3} \text{ s}^{-1},$$

but if the 200 m transition zone delineated by Shapiro (1984) is used with the same velocity difference, the cross-front shear will be an order of magnitude larger. Consequently, it does not seem inappropriate to use the model solutions of Part I to provide estimates of frontal dissipation.

Three evaluations are considered, corresponding to different values of the diffusion coefficient. The basic model results are reviewed, and the dissipation of both kinetic energy and enstrophy are defined in section 2. The magnitudes of kinetic energy dissipation are presented in section 3 and found to be 1–2 orders of magnitude larger than local dissipation rates associated with both clear air turbulence and the planetary boundary layer. The dissipation of enstrophy is compared to enstrophy production in section 4. An essential balance may be achieved when the diffusion coefficient is relatively small, but the expansion of the frontal zone associated with large values of the diffusion coefficient is also accompanied by relatively large enstrophy dissipation compared to production. The final remarks emphasize the need to consider both theoretical constraints and observations to account for dissipation in frontal zones in numerical circulation models.

2. Solution and model analysis

Frontal zone dissipation will be determined from the semigeostrophic Eady-wave solution for the alongfront velocity component v derived in Part I (section 3 and Appendix). Traditional geostrophic scales are used to represent the solution in nondimensional form. The dependent variable is expressed as

$$v(x, z, t) = V(x, z, \tau)Ae^{\sigma t}, \tag{1}$$

where the waveform V is periodic along the horizontal axis, defined in the domain $-\pi \leq x \leq \pi$, (the x-coordinate is defined as the nondimensional product kx) and the wave is contained in a vertical channel, $-0.5 \leq z \leq 0.5$. Time is represented by t and by a modified time variable defined as

$$\tau = kA \text{ Ro}e^{\sigma t}, \tag{2}$$

where the wavenumber and growth rate of the most unstable Eady wave are provided by $(k, \sigma) = (1.6061, 0.3098)$ and $\text{Ro} = U/fL \leq 0.3$ is the Rossby number (the basic flow and alongfront velocity scale is U, the

quarter wavelength is L and f is the Coriolis parameter). The initial wave amplitude A is given by

$$A = ak\left[\left(\frac{b}{a}\right)^2 \sinh^2 kz + \cosh^2 kz\right]^{1/2}, \quad (3)$$

where the parameter values are $a = 0.05$ and $b/a = 1.5021$ and, for these values, the dimensional amplitude is less than 5 m s^{-1}.

The inviscid Eady wave is modified by embedding a thin dissipative layer into the solution that is intended to model a frontal zone. Imposition of this layer, which models momentum diffusion, smooths out the discontinuity in v (infinite relative vorticity) that forms at $\tau = 1$. Moreover, momentum diffusion counteracts amplitude growth associated with baroclinic instability, enabling the wave amplitude to attain a relatively steady state or a state where the wave decays in amplitude. The ultimate state depends on the magnitude of the nondimensional diffusion coefficient ϵ.

The composite solution for the periodic variable V defined in (1), is given by [Part I, Eqs. (10) and (11)]:

$$V = V_1 + H(\tau)\left\{\tanh\left[\frac{H(\tau)}{2\epsilon}(x+\delta)\right] - 1\right\} \quad (4a)$$

for $0 \leqslant x + \delta \leqslant \pi$, and by

$$V = V_1 - |H(\tau)|\left\{\tanh\left[\frac{-|H(\tau)|}{2\epsilon}(x+\delta)\right] - 1\right\} \quad (4b)$$

for $-\pi \leqslant x + \delta \leqslant 0$. The height dependent phase $\delta(z)$ is defined in Part I (18b). The function V_1, defined by

$$V_1 = \sin(x + \delta + V_1\tau), \quad (5)$$

and the function H defined by

$$H(\tau) = \beta/\tau < 1, \quad (6)$$

where $\beta^{-1}\sin\beta = \tau^{-1} < 1$, are evaluated for $\tau > 1$. This solution, represented by (4)–(6), is composed of an inviscid part represented by V_1, and a dissipative part characterized by amplitude $|H(\tau)|$ and frontal half-width of order 2ϵ. The composite solution provides a model of a front in the (x, z) plane that does not exhibit discontinuous behavior. Some characteristic solutions are displayed in Figs. 2–5 of Part I.

The solution for V that is appropriate when $(2\epsilon)^{-1} \gg \tau \gg 1$ reduces to [Part I, Eq. (17)]:

$$V = \frac{1}{1+\tau}\left\{\pi \tanh\left[\frac{\pi(x+\delta)}{2\epsilon(1+\tau)}\right] - (x+\delta)\right\}. \quad (7)$$

This relatively simple form of the solution represents a baroclinic wave that has reached equilibration because the alongfront velocity satisfies $v \propto V\tau$, which follows from (1) and (2). The significant aspect of this solution for present purposes is the fact that this asymptotic solution (7) satisfies Burgers equation

$$\frac{\partial V}{\partial \tau} - V\frac{\partial V}{\partial x} = \epsilon\frac{\partial^2 V}{\partial x^2}, \quad (8)$$

which may be verified by substitution. It is convenient, for present purposes, to represent (8) in terms of the along-front velocity v. The transformation may be accomplished by use of (1) and (2) to yield

$$\frac{\partial v}{\partial t} - \sigma k\,\mathrm{Rov}\frac{\partial v}{\partial x} - \sigma v = \epsilon\sigma\tau\frac{\partial^2 v}{\partial x^2}. \quad (9)$$

Temporal changes in v occur by three different processes: 1) nonlinear self-advection steepens the waveform, 2) baroclinic instability provides exponential amplitude growth, and 3) momentum diffusion or eddy viscosity counteracts both wave steepening and growth of the wave amplitude. Although amplitude equilibration is represented by (7), momentum diffusion overcompensates the steepening process and the transitional zone-expands with time.

An analysis of frontal dissipation may be formulated by means of (9). The frontal zone will be defined as the distance Δx between the minima and maxima of v (see Part I, Figs. 3 and 6). Multiplication of (9) by v followed by integration over the width of the frontal zone, denoted by a bar, yields the equation for the time rate of change of kinetic energy:

$$\frac{1}{2}\frac{\partial}{\partial t}\overline{v^2} = \frac{1}{2}\sigma k\,\mathrm{Rov}\,\overline{\frac{\partial v^2}{\partial x}} + \sigma\overline{v^2} - \epsilon\sigma\tau\overline{\left(\frac{\partial v}{\partial x}\right)^2}. \quad (10)$$

The dissipation of kinetic energy over one-half the fluid depth (approximately 5 km) is defined as

$$\mathrm{DKE} = \epsilon\sigma\tau\int_{-0.5}^{0}\frac{1}{\Delta x}\int_{-\Delta x/2}^{\Delta x/2}\left(\frac{\partial v}{\partial x}\right)^2 dx\,dz. \quad (11)$$

Evaluation of (11) will be deferred until the following section.

Next, an equation for the relative vorticity $\partial v/\partial x$ is derived from (9). Multiplication of this vorticity equation by $\partial v/\partial x$ and integration across the frontal zone yields an equation for the time rate of change of the enstrophy:

$$\frac{1}{2}\frac{\partial}{\partial t}\overline{\left(\frac{\partial v}{\partial x}\right)^2} = \sigma\overline{\left(\frac{\partial v}{\partial x}\right)^2} + \frac{1}{2}\sigma k\,\mathrm{Ro}\overline{\left(\frac{\partial v}{\partial x}\right)^3} - \epsilon\sigma\tau\overline{\left(\frac{\partial^2 v}{\partial x^2}\right)^2}. \quad (12)$$

The first two terms on the right-hand side of (12) represent production of enstrophy. The first term represents amplitude growth as a consequence of baroclinic instability, the counterpart of $\sigma\overline{v^2}$ in (10). The second term, the *skewness*, represents enstrophy production as nonlinear self-advection steepens the waveform: in the absence of enstrophy dissipation, the enstrophy be-

comes infinite with the development of a discontinuity in v. The vertically integrated skewness and enstrophy dissipation are defined as

$$\text{SKEW} = \frac{1}{2}\sigma k \,\text{Ro} \int_{-0.5}^{0} \frac{1}{\Delta x} \int_{-\Delta x/2}^{\Delta x/2} \left(\frac{\partial v}{\partial x}\right)^3 dxdz, \quad (13)$$

and

$$\text{DEN} = \epsilon\sigma\tau \int_{-0.5}^{0} \frac{1}{\Delta x} \int_{-\Delta x/2}^{\Delta x/2} \left(\frac{\partial^2 v}{\partial x^2}\right)^2 dxdz. \quad (14)$$

Both production SKEW and dissipation DEN of enstrophy will be considered in section 4.

3. Kinetic energy dissipation in a frontal zone

a. Results

The evaluation of (11) proceeds as follows. Expressions (1) and (2) are introduced into (11) to yield

$$\text{DKE} = \sigma(\text{Ro}k)^{-2} D, \quad (15)$$

where the dissipation integral is defined as

$$D = \epsilon\tau^3 \int_{-0.5}^{0} \frac{1}{\Delta x} \int_{-\Delta x/2}^{\Delta x/2} \left(\frac{\partial V}{\partial x}\right)^2 dxdz. \quad (16)$$

The nondimensional dissipation DKE is scaled by U^3HL^{-1}, where U is the magnitude of the zonal velocity and H and L are, respectively, vertical and horizontal scales associated with the Eady wave. The coefficient of D, in (13) has also been scaled by means of U and L. Consequently, the *dimensional* expression for the dissipation, expressed in W m^{-2}, becomes

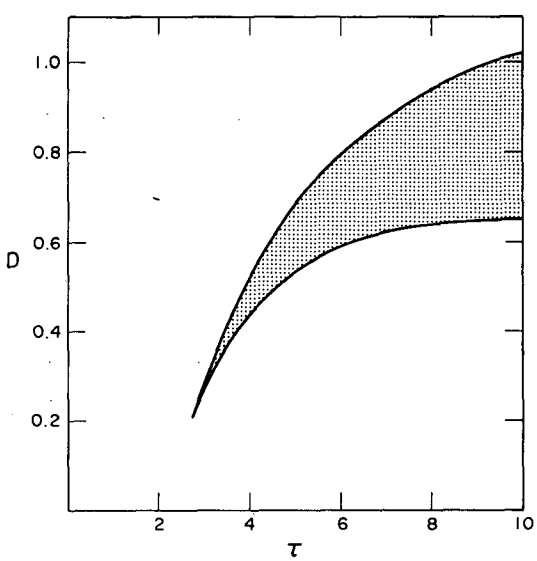

FIG. 1. Dissipation integral (16) expressed as a function of modified time τ (see Table 1). The stippled region represents values of D that occur when $10^{-2} \leq \epsilon \leq 10^{-1}$. The upper and lower curves are, respectively, $\epsilon = 10^{-2}$ and $\epsilon = 10^{-1}$.

TABLE 1. Values of τ at $|z| = 0.5$ and corresponding times $t(d)$ for Ro = 0.2 and Ro = 0.3.

	τ					
	1.00	2.37	4.00	6.00	8.00	10.00
$t\|_{\text{Ro}=0.2}$	5.64	7.25	8.22	8.99	9.52	9.94
$t\|_{\text{Ro}=0.3}$	3.25	4.33	4.98	5.49	5.84	6.12

$$\rho\text{DKE} = \rho\sigma(fk^{-1})^2 HD \quad (17)$$

where (σ, k, f) are dimensional quantities and ρ is a mean density of the lower 5-km layer. The characteristic magnitude of the dissipation will be considered below.

The variation of D is presented as a function of τ in Fig. 1. The dimensional times t, associated with τ, appear in Table 1. The dissipation range is bounded from above by $\epsilon = 10^{-2}$ and from below by $\epsilon = 10^{-1}$. The dissipation increases to keep pace with the exponential amplitude growth, but then tends to level off as momentum diffusion becomes dominant.

The dependence of the dissipation integral on the parameters (ϵ, τ) may also be displayed for $(2\epsilon)^{-1} \gg \tau \gg 1$ by use of (7) to evaluate (16). In this case (7) is used to evaluate the total dissipation over one wavelength, defined as

$$D' = \epsilon\tau^3 \int_{-0.5}^{0} \frac{1}{2\pi} \int_{-\pi}^{\pi} \left(\frac{\partial V}{\partial x}\right)^2 dxdz. \quad (18)$$

The expression determined by integration over one wavelength is

$$D(2\pi) = \frac{\pi^3}{3}\left(\frac{\tau}{1+\tau}\right)^3 - \epsilon\tau\left(\frac{\tau}{1+\tau}\right)^2. \quad (19)$$

The purpose of this evaluation is to provide confirmation that essentially all the dissipation occurs in the transition zone of width Δx. The results are displayed in Table 2. The parameter τ decreases with height z

TABLE 2. Comparison between the dissipation defined by (16) and the dissipation defined by (18). The expression that is appropriate for τ large (7) is used to evaluate (18). $D = \int_{-0.5}^{0} D(\Delta x)dz$ and $D' = \int_{-0.5}^{0} D(2\pi)dz$.

z	τ	$D(\Delta x)$	$D(2\pi)$
−0.50	10.00	2.381	2.389
−0.45	9.17	2.326	2.337
−0.40	8.41	2.268	2.281
−0.35	7.72	2.206	2.222
−0.30	7.11	2.142	2.162
−0.25	6.58	2.016	2.102
−0.20	6.13	2.016	2.045
−0.15	5.76	1.960	1.993
−0.10	5.50	1.916	1.954
−0.05	5.33	1.886	1.926
0.00	5.28	1.876	1.918
		$D = 1.025$	$D' = 1.058$

because the amplitude A, defined by (3), is a decreasing function of z in $-0.5 \leq z \leq 0$. The third column contains the numerical evaluation over the transition region, and the fourth column contains an evaluation of (19). The values at the bottom of these columns represent (16) and (18). In this case, $\epsilon = 0.01$, the differences are negligible. However, for larger values of ϵ the relative differences range from 10–15 percent.

b. Discussion

The magnitude of the dissipation may be found from (17). Characteristic values of the parameters are: $\rho \approx 1$ kg m^3, $H \approx 10^4$ m, $f \approx 10^{-4}$ s^{-1}, $k \approx 1.61 \times 10^{-6}$ m^{-1} and $\sigma = 0.62 \times 10^{-5}$ s^{-1}. The characteristic magnitude of the dissipation is

$$\rho \mathrm{DKE} \approx 240 D \quad [\mathrm{W\ m^{-2}}].$$

Consequently, the dissipation associated with the parameter range in Fig. 1 is in the range of 50–250 W m^{-2}.

As noted in the Introduction, a dissipation of 75 W m^{-2} characterized an upper level front examined by Kennedy and Shapiro (1980). These values are relatively large when compared to dissipation of 1–5 W m^{-2} in clear air turbulence and in the planetary boundary layer. However, suppose a value of 1 W m^{-2} is considered as an average value in the planetary boundary layer. Then the total global dissipation is 5.1×10^{14} W. To place frontal dissipation in perspective, consider that the area that encompasses the frontal dissipation is $10^5 \times 10^6$ m^2, which yields a total frontal dissipation of about (250 W m^{-2}) (10^{11} m^2) $\approx 0.25 \times 10^{14}$ W. Consequently, an equivalent global dissipation would require the presence of at least 20 midlatitude fronts. This number of fronts is in excess of the number that would exist in midlatitudes in winter. Moreover, the value of 250 W m^{-2} used for this evaluation may not be a representative value, since not all fronts would be in a mature stage.

A conclusion that may be drawn from the present model calculation is that midlatitude surface fronts make a nonnegligible contribution to global dissipation of kinetic energy. However, local dissipation during the life cycle of a cyclone may be one to two orders of magnitude larger than that associated with both clear air turbulence and the planetary boundary layer.

4. Enstrophy dissipation in a frontal zone

Evaluation of (13) and (14) proceeds as in the evaluation of kinetic energy dissipation. Expressions (1) and (2) are introduced into (13) and (14) to yield the skewness

$$\mathrm{SKEW} = \sigma(\mathrm{Ro}k^{-2})S, \tag{20}$$

and the enstrophy dissipation

$$\mathrm{DEN} = \sigma(\mathrm{Ro}k^{-2})N. \tag{21}$$

The skewness (or enstrophy production) and the enstrophy dissipation integrals are defined, respectively, as

$$S = \frac{1}{2}\tau^3 \int_{-0.5}^{0} \frac{1}{\Delta x} \int_{-\Delta x/2}^{\Delta x/2} \left(\frac{\partial V}{\partial x}\right)^3 dxdz. \tag{22}$$

$$N = \epsilon\tau^3 \int_{-0.5}^{0} \frac{1}{\Delta x} \int_{-\Delta x/2}^{\Delta x/2} \left(\frac{\partial^2 V}{\partial x^2}\right)^2 dxdz. \tag{23}$$

As in the case of kinetic energy dissipation, almost all the production and dissipation of enstrophy occurs in the transitional zone Δx. Since a discontinuity in the relative vorticity is prevented by the inclusion of dissipation, S cannot exceed N. The relative magnitudes of these integrals are shown in Fig. 2. The essential balance between production and dissipation, that characterizes the curve for $\epsilon = 10^{-2}$, provides another confirmation of the equilibration that characterizes the v-field (Figs. 2 and 8 in Part I). The relatively larger enstrophy dissipation that characterizes the curves for $\epsilon = 5 \times 10^{-2}$ and $\epsilon = 10^{-1}$ is also reflected in the expansion of the transitional zone in Figs. 4 and 5 of Part I.

5. Final remarks

Frontal dissipation has been evaluated by means of a semigeostrophic model. The results apply to the dissipation occurring within a narrow transition zone, small compared to the wavelength of an unstable Eady wave. The global dissipation of kinetic energy in midlatitude frontal zones does not appear to be as large as dissipation in the planetary boundary layer: the relative magnitudes remain an open question. Yet the present model results, as well as the dissipation determined in an upper tropospheric frontal zone by Kennedy and

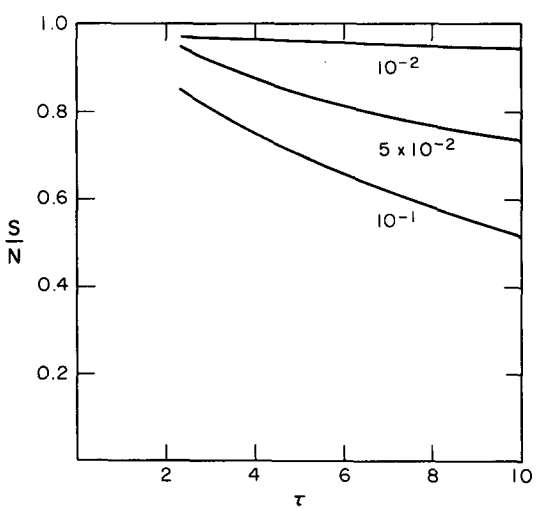

FIG. 2. Ratio of enstrophy production S to enstrophy dissipation N as a function of modified time τ (see Table 1). Values of ϵ that are associated with each curve appear in the figure.

Shapiro (1980), reveal that local dissipation rates are far in excess of values that characterize both clear air turbulence and planetary boundary layer dissipation.

The present values may represent overestimates of dissipation rates within the frontal zone itself. Thorpe (1973), for example, examined the development of turbulence within a stratified layer by Kelvin–Helmholtz instability. Thorpe (section 5) found that only about 5 percent of the turbulent energy is lost to internal gravity waves, generated at the edge of the turbulent region, in his laboratory experiment. Yet he suggests that "energy lost by internal wave radiation is possibly significant in the atmosphere." Although this conjecture and the reality of large local dissipation rates have yet to be established by observational studies, the incorporation of frontal dissipation into numerical circulation models in a physically correct manner merits consideration.

The cascade process that is described by the present frontal model is similar to that occurring in shock wave formation as described by Saffman (1968). Energy is transferred to small scales where it is dissipated as in the theory of homogeneous turbulence. However, as Saffman points out, the larg-scale motion does not uncouple from the dissipative scales: "the formation of large gradients of $\partial v/\partial x$ is the cascade and it depends on the large-scale motion." As a consequence, the spectral decay should *not* exhibit the minus five-thirds x-wavenumber dependence that characterizes homogeneous turbulence. In fact, Andrews and Hoskins (1978) and Platzman (1964) have shown that the inviscid form of (8) predicts a minus eight-thirds dependence at the time when $\partial v/\partial x = \infty$. Dissipation modifies the spectrum such that when the solution may be represented by (7), the spectral decay is exponential for large values of the wavenumber; e.g., Lesser and Chrighton (1975). Examination of characteristic frontal spectra as well as examinations of the roles of moist convection and of gravity waves in frontal dissipation remain as a future challenge.

Acknowledgments. Financial support for this investigation has been provided by the National Science Foundation under NSF Grant ATM-8820164. Thanks are expressed to Helen Jones who carried out all the numerical computations on the Pyramid 90X super minicomputer at the University of Colorado Center for Atmospheric Theory and Analysis.

REFERENCES

Andrews, D. G., and B. J. Hoskins, 1978: Energy spectra predicted by semi-geostrophic theories of frontogenesis. *J. Atmos. Sci.*, **35,** 509–512.

Blumen, W., 1980: A comparison between the Hoskins-Bretherton model of frontogenesis and the analysis of an intense frontal zone. *J. Atmos. Sci.*, **37,** 64–77.

——, 1990: A semigeostrophic Eady-wave frontal model incorporating momentum diffusion: Part I. Model and solutions. *J. Atmos. Sci.*, **47,** 2890–2902.

Brümmer, B., 1988: Structure and circulation in the boundary layer at a strong front. *Beitr. Phys. Atmos.*, **61,** 232–243.

Gall, R. L., R. T. Williams and T. L. Clark, 1987: On the minimum scale of surface fronts. *J. Atmos. Sci.*, **44,** 2562–2574.

——, —— and ——, 1988: Gravity waves generated during frontogenesis. *J. Atmos. Sci.*, **45,** 2204–2219.

Hess, S. L., 1959: *Introduction to Theoretical Meteorology.* Holt, Rinehart and Winston, 362 pp.

Hoskins, B. J., 1982: The mathematical theory of frontogenesis. *Ann. Rev. Fluid Mech.*, **14,** 131–151.

Kennedy, P. J., and M. A. Shapiro, 1975: The energy budget in a clear air turbulence zone. *Mon. Wea. Rev.*, **103,** 650–654.

——, and ——, 1980: Further encounters with clear air turbulence in research aircraft. *J. Atmos. Sci.*, **37,** 986–993.

Lesieur, M., 1987: *Turbulence in Fluids.* Martinus Nijhoff Publishers, 286 pp.

Lesser, M. B., and D. G. Chrighton, 1975: Physical acoustics and the method of matched asymptotic expansions. *Phys. Acoust.*, **11,** 69–149.

Lilly, D. K., and P. F. Lester, 1974: Waves and turbulence in the stratosphere. *J. Atmos. Sci.*, **31,** 800–812.

Nakamura, N., and I. M. Held, 1989: Nonlinear equilibration of two-dimensional Eady waves. *J. Atmos. Sci.*, **46,** 3055–3064.

Platzman, G. W., 1964: An exact integral of complete spectral equations for unsteady one-dimensional flow. *Tellus,* **16,** 422–431.

Saffman, P. G., 1968: Lectures on homogeneous turbulence. *Topics in Nonlinear Physics,* N. J. Zabusky, Ed., Springer-Verlag, 485–614.

Shapiro, M. A., 1984: Meteorological tower measurements of a surface cold front. *Mon. Wea. Rev.*, **112,** 1634–1639.

Thorpe, S. A., 1973: Turbulence in stably stratified fluids: a review of laboratory experiments. *Bound.-Layer Meteor.*, **5,** 95–119.

——, 1987: Transitional phenomena and the development of turbulence in stratified fluids. *J. Geophys. Res.*, **92,** 5231–5248.

Trout, D., and H. A. Panofsky, 1969: Energy dissipation near the tropopause. *Tellus,* **21,** 355–358.

Young, G. S., and R. H. Johnson, 1984: Meso- and microscale features of a Colorado cold front. *J. Climate Appl. Meteor.*, **23,** 1315–1325.